J Solid State Electrochem (2007) 11:531–542
DOI 10.1007/s10008-006-0190-3

ORIGINAL PAPER

Hybrid organic/inorganic films of conducting polymers modified with phthalocyanines. II. EIS studies and film characterization

Ahmed Galal · Soher A. Darwish · Rasha A. Ahmed

Received: 22 April 2006 / Revised: 2 May 2006 / Accepted: 20 June 2006 / Published online: 6 September 2006

Abstract Conducting polymers were modified with Cu-phthalocyanine or Co-phthalocyanine embedded in a sol–gel matrix. The resulting films were characterized using electrochemical impedance spectroscopy, Fourier transform infrared spectroscopy and scanning electron microscopy. Electrochemical impedance spectroscopy data showed that the application of the sol–gel layer to the conductive polymer caused a noticeable increase in the impedance of the film across the frequency ranges studied. The hydrophobic character of the film was greatly influenced by the sol–gel and caused an increase in its capacitance. A modified 'Randles' equivalent cell was used to correlate the electrochemical parameters of the films. Elemental analysis and infrared data confirmed the presence of the phthalocyanine moieties in the film and the empirical formula of the film was estimated. The surface morphology of the sol–gel-modified conducting polymer was distinctly amorphous compared to the poly(3-methyl thiophene).

Keywords Conducting polymers · Metal-phthalocyanines · Hybrid organic/inorganic composites · EIS · FTIR · SEM

Introduction

Conductive polymer films have been widely used in several applications; electrode modification has been one of the most attractive in the last few decades [1, 2]. The modification of the conductive polymer with inorganic complexes has attracted special interest to produce hybrid composite films [3]. Transition metal-based phthalocyanines (Pcs) are of particular importance in the areas of fuel cells, gas sensors, and biosensors. Most of these applications require the use of Pcs in the form of thin films. The deposition of platinum-Pc on platinum, glassy carbon, and gold by dry abrasion was investigated using electrochemical techniques [4]. The polymer produced has good electronic contact and adhesion between the micro-crystals and the electrode. Other methods were also used to modify solid surfaces with Pcs, such as vacuum-deposited CuPc on conducting poly(pyrrole) films [5]. The crystalline nature and morphology of the Pc films were affected by the substrate preconditioning before film deposition [6]. Sono-gel-carbon-poly(thiophene) micro-structured electrode has been synthesized by sono-catalytic technique [7]. The entrapment of the polymer inside a composite material drastically enhances the stability of the redox-active phase towards irreversible oxidation. Thus, it was possible to develop voltammetric sensors based on electrodes chemically modified with electroactive substances of conducting polymers and Pc complexes with improved cross-selectivity [8]. In another example, the electrochemical oxidation of NADH was investigated at a glassy carbon electrode modified with electropolymerized films of metal Pc [9].

Pc moieties could be incorporated in film matrices with different approaches, for example, iron tetrasulfo-Pc was incorporated in sol–gel materials directly during the synthesis of hydrophobic and hydrophilic sol–gel materials by three different methods [10]. The electrochemical response of metal/electroactive polymer–film/solution system to a low-amplitude variation of electrode polarization was extensively studied [11]. The charge-diffusion transport of electronic and ionic species in the bulk film and non-equilibrium heterogeneous charge transfer was determined,

A. Galal (✉) · S. A. Darwish · R. A. Ahmed
Department of Chemistry, College of Science,
University of Cairo,
1 Al Gamaa Street,
12613 Giza, Egypt
e-mail: galalah1@yahoo.com

and it was concluded that electrons are exchanged at the metal–film boundary and ions at the film–solution interface.

On the other hand, spectroscopic methods were also used to characterize hybrid films. Thus, polymeric (octacyano phthalocyaninato polysiloxane) has been characterized by infrared (IR), UV–Vis spectroscopy, elemental analysis, and electron spectroscopy for chemical analysis [12]. Surface studies using scanning electron microscopy (SEM) proved to be useful in identifying the relation between the film morphology and its electrochemical characteristics [13, 14]. In the first part of this work [41], we showed that hybrid films of conductive polymer and metal-Pc could be prepared by different methods. In this paper, we studied the electrochemical impedance characteristics of a hybrid film formed of poly(3-methyl thiophene), PMT, and a metal-Pc (MPc). The data obtained from elemental analysis, spectroscopic measurements, and SEM will be presented and related to the electrochemical characteristics of the film.

Experimental

Chemicals and electrochemical cells

All chemicals were used without further purification. 3-Methylthiophene (MT), tetrabutyl ammonium tetrafluoroborate (TBATFB), acetonitrile (AcN), tetraethyl orthosilicate, ferric nitrate, and potassium ferricyanide were obtained from Aldrich (Milwaukee, WI, USA). Other chemicals were purchased from Merk (Munich, Germany). Aqueous solutions were prepared by dilution from stock solutions using double-distilled water.

Electrochemical polymerization and characterizations were carried out in a three-electrode/one-compartment glass cell. The details of electrodes used in electrochemical impedance spectroscopy (EIS) measurements and their polishing procedures were mentioned previously [41]. 'Puratronic' Pt wire was used to prepare samples for SEM examination. All potentials in this study were referenced to 3M Ag/AgCl. Highly purified nitrogen was used for oxygen removal by bubbling. All experiments were performed at 25±0.2 °C.

Equipment and techniques

The electrosynthesis of the polymers and their electrochemical characterization were performed using a BAS-100B electrochemical analyzer (BAS, West Lafayette, IN, USA). The polymer films were electrochemically deposited as indicated earlier [41].

EIS measurements were performed using a Gamry-750 system, a lock-in-amplifier and the system is connected to a personal computer. EIS was performed in monomer free electrolytes as indicated. The data analysis software was provided with the instrument and applied nonlinear least-square filling with Levenberg–Marquardt algorithm. The measurements were performed under potentiostatic control at different applied potentials. The working electrode was conditioned before running the experiment to ensure current stabilization. The constant applied potentials were decided from the polarization experiment recorded for the film in the test electrolyte. All impedance experiments were recorded between 10 mHz and 100 kHz with an ac excitation signal of 10 mV amplitude.

Phthalocyanine application to the polymer

Conductive polymer modification with MPc was achieved according to the following procedure: A solution was prepared by mixing 10% $FeCl_2$, formamide, ethanol, and 0.1 M nitric acid. The solution was then used for dip coating the electrode. In the case when Cu- or Co-Pc was mixed with this solution, an addition of 0.5 wt% was used. Further treatment of the film and details were as described previously [41].

Results and discussion

Electrochemical impedance spectroscopy of unmodified conducting polymer film

Electrochemical impedance spectroscopy is a valuable technique for determining important characteristics of electrochemically active polymer materials [15]. The analysis of impedance data allows obtaining information on charge transfer resistance, double layer and limiting capacitances at low frequency, diffusion coefficients and, provided the reaction mechanism is known, exchange current densities [16]. Therefore, it was important to perform EIS measurements to understand the changes imparted to the PMT film when modified with the sol–gel (MPc) layer.

The potential dependence of impedance spectrum for PMT formed at constant applied potential, E_{app}=1.75 V for 30 s, in 0.1 M H_2SO_4 is shown in Fig. 1. The results are presented in the form of Bode plot that will allow a more effective extrapolation of data at relatively high frequencies. The values of the constant potential applied to the polymer film during impedance measurements were selected within a relatively wide range, ca. 0.0–1.1 V. It is important to notice that the polymer film starts to develop electronic/ionic conductivity as the applied potential approaches its oxidation around +0.6 V (in non-aqueous media) and +0.4 V (in aqueous media) [17]. The measured

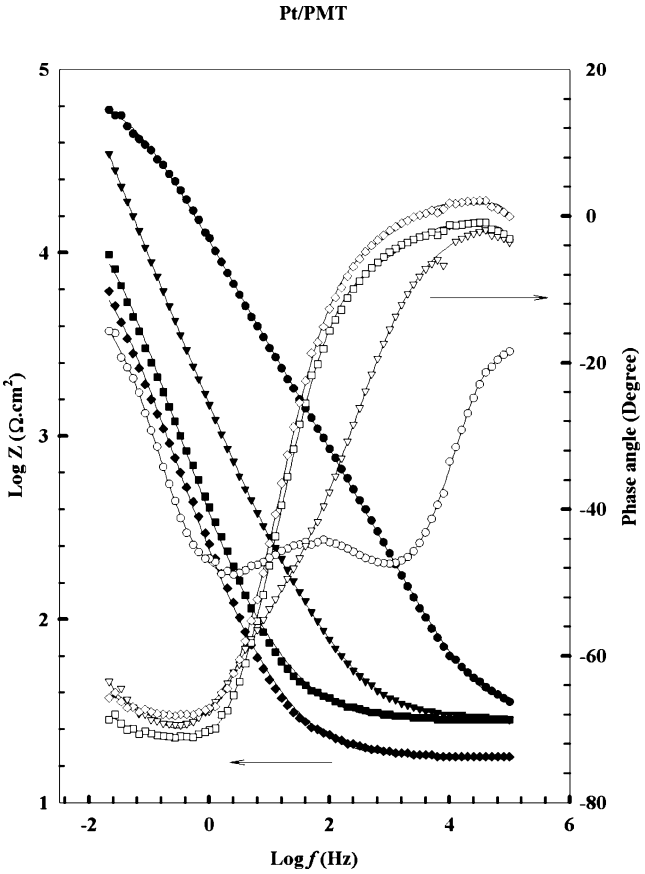

Fig. 1 Bode plots of PMT films prepared (from 0.05 3MT, 0.1 M TBATFB/AcN) under potentiostatic conditions for 30 s (E_{app}=1.75 V) in 0.1 M H_2SO_4. Data are shown for different dc voltages of 0.0 (▾), 0.4 (∩), 0.7 (▾), and 1.1 V (▾), respectively. *Dark symbols* represent log Z vs log f and *open symbols* represent phase angle vs log f relations. *Solid lines* represent simulated data based on the parameters of equivalent circuits of Fig. 5

values of direct current electronic conductivity (σ) in PMT clearly indicated that electronic transport is fast in this system in a given potential window [18]. It is also well established that the main carriers for charge transport are bi-polarons in poly(thiophene) systems [19]. The value of potential at which the maximum value of σ is achieved corresponds to the maximum spin content of the polymer [20]. In this consideration, the estimation of the polymer resistance (R_{poly}) is based on the fact that the film is a semi-infinite system [21]. The EIS data of Fig. 1 are for a film with an estimated thickness of 250 nm if we consider that polymer film deposition takes place with 100 mC cm^{-2} passing in the electrochemical cell.

Examining the impedance spectra for this film shows that the electronic resistance of PMT, estimated from Ohm's law (ca. in the order of 1.0×10^{-3} Ω), will be neglected. Thus, the differences in the EIS data of PMT doped with the supporting electrolyte-anion reveal mainly the onset of a capacitive behavior as the frequency increases. As would be expected, the ohmic resistance, R_Ω, dominates the impedance at the high frequency 'horizontal' plateau. On the other hand, at relatively low frequencies, polarization resistance (R_p) also contributes, and the values of ($Rp + R_\Omega$) can be read at the low-frequency end. The departure from the constant phase element (CPE) shows varying slopes as the applied dc voltage, E_{app}, changes. Thus, a near-90° capacitive line that extends to relatively low frequencies as E_{app} exceeds +0.4 V dominates the impedance plots. The latter case is where the polymer film is expected to achieve fully doped/conductive state. This observation is in good agreement with the results described previously in the literature for conducting polymers in similar potential ranges [22, 23]. According to the model described by Pickup [23], the ionic resistance, R_{ion}, of the polymer film was obtained from the EIS data. As shown in Fig. 1, the slopes of the linear part in the intermediate range of frequency are about the same for the potential range higher than 0 V. The electrolytic resistance, $R_{electrol}$, is estimated from the high-frequency intercept, as indicated earlier. The direct current resistance of the polymer, R_{poly}, is relatively lower than that of the electrolytic solution, $R_{electrol}$. The electrolytic resistance is in the range of 60–100 Ω (from conductance measurements). In the potential range in which the films acquire a high level of doping, R_{poly} is <10 Ω (from four probe measurements) [18]. The presence of relatively small anionic species, in this case SO_4^{2-}, allows their uptake by the polymeric film during the oxidation process [24]. As the applied potential to the polymer film shifts towards more positive values, ionic transport became more pronounced compared to electronic transport within the film. This is clearly noticed again in the slight change in the slope of the impedance curves of Fig. 1 for E_{app}=0.4, 0.8, and 1.1 V. An explanation for this trend is the increase in the anion uptake by the film as the applied potential increases. Moreover, the increase of charge delocalization in the oxidized polymeric chains and the consequent change of solvation energy for the doping anions contribute to the previously mentioned effect.

Electrochemical impedance spectroscopy of conducting polymer/sol–gel and polymer/sol–gel(MPc) films

For sol–gel modified films formed as indicated in the "Experimental" section by applying a sol–gel coating to the conducting polymer layer, a noticeable increase in the impedance of the film in the low-, intermediate-, and high-frequency regions were observed as shown in Fig. 2 (the corresponding data for the conducting polymer/sol–gel (Cu- and Co-Pc) films are given in Figs. 3 and 4, respectively). At relatively higher applied potentials, ca. near the doping process of the films, the increase in the resistive behavior of the film for the charge transfer is even more pronounced. On the other hand, the capacitive

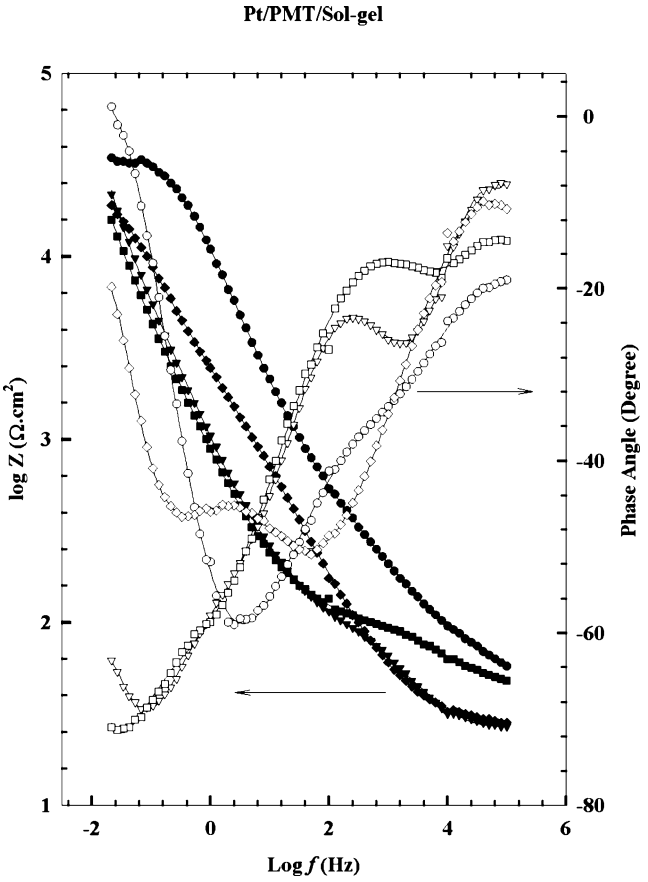

Fig. 2 Bode plots of PMT films prepared (from 0.05 3MT, 0.1 M TBATFB/AcN) under potentiostatic conditions for 30 s (E_{app}=1.75 V) in 0.1 M H_2SO_4 and modified with a sol–gel layer. Data are shown for different dc voltages of 0.0 (▾), 0.4 (∩), 0.7 (▾), and 1.1 V (▾), respectively. *Dark symbols* represent log *Z* vs log *f* and *open symbols* represent phase angle vs log *f* relations. *Solid lines* represent simulated data based on the parameters of equivalent circuits of Fig. 5

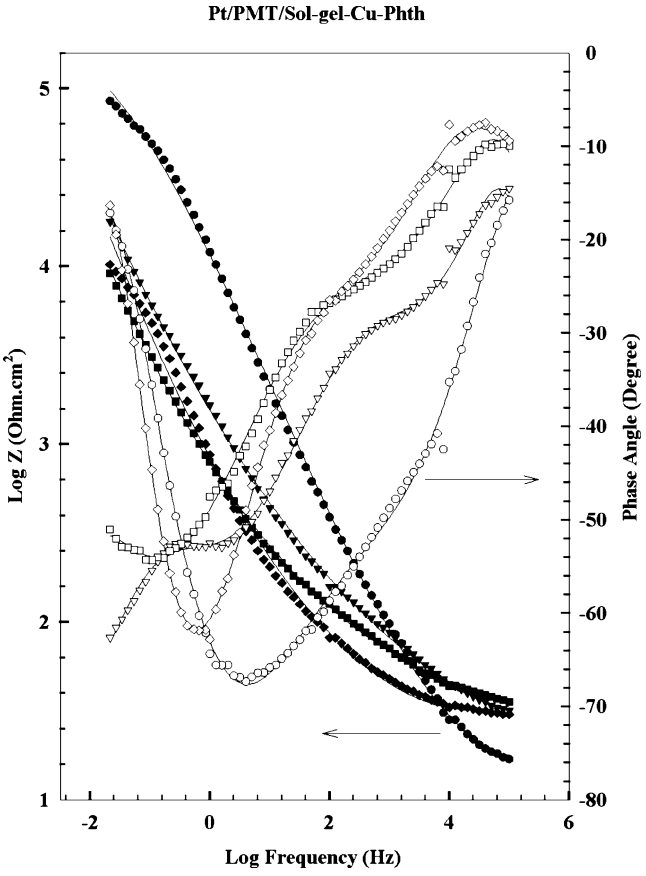

Fig. 3 Bode plots of PMT films prepared (from 0.05 3MT, 0.1 M TBATFB/AcN) under potentiostatic conditions for 30 s (E_{app}=1.75 V) in 0.1 M H_2SO_4 and modified with a sol–gel containing Cu-phthalocyanine layer. Data are shown for different dc voltages of 0.0 (▾), 0.4 (∩), 0.7 (▾), and 1.1 V (▾), respectively. *Dark symbols* represent log *Z* vs log *f* and *open symbols* represent phase angle vs log *f* relations. *Solid lines* represent simulated data based on the parameters of equivalent circuits of Fig. 5

behavior in the intermediate-frequency region is also noticeably observed as compared to the same region of the unmodified polymer film (cf. Fig. 1). From the above, two important observations are noticed: (1) for partially doped films, i.e., those subjected to an E_{app}=0.4 V, at higher frequencies there is a resistance followed by diffusion and capacitive components as the frequency decreases, and (2) as the E_{app} increases to a value where the doping level of the polymer increases, the impedance is dominated by the capacitive behavior. The latter phenomenon is more pronounced in the case of sol–gel modified films. With the potential used and the grafted sol–gel layer on the conductive film, the surface roughness is expected to be high for the resulting thickness of the hybrid film. The phase angle relation with frequency for the Pt/PMT/sol–gel film shows a variation in the intermediate-frequency range indicating that more than one time constant should be expected for charge transfer in this case. Moreover, it should be expected that ionic diffusion through the sol–gel layer is more predominant at the film/electrolyte interface. This is again a noticeable impedance behavior at the high-frequency end of the EIS diagram.

The total resistance (R_t) consists of a high frequency resistance (R_{hf}) that corresponds to the electrolyte resistance ($R_{electrol}$) in series with the polymer resistance (R_{poly}). The low-frequency resistance (R_{lf}) associated with the capacitance (C_{ox}) of the oxidized polymer can be deduced as follows:

$$R_{hf} = R_{electrol} + R_{poly} \quad (1)$$

$$R_t = R_{electrol} + R_{poly} + R_{lf} \quad (2)$$

Equation (1) is used to determine the electrolytic resistance, $R_{electrol}$, when the film is fully oxidized and its resistance could be neglected.

The faradaic impedance data for several conducting polymers such as poly(pyrrole) [25], poly(aniline) [26], and

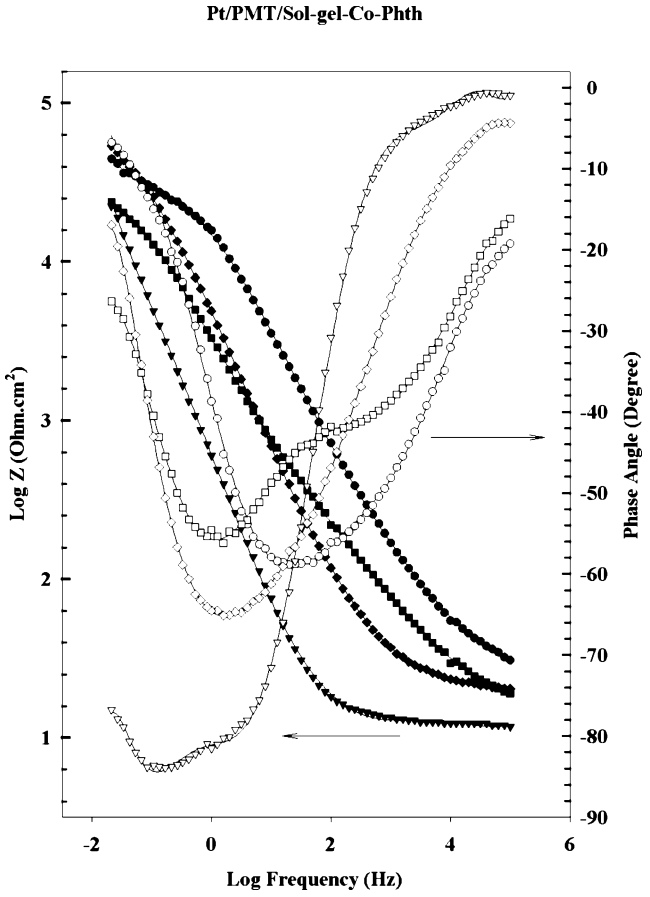

Fig. 4 Bode plots of PMT films prepared (from 0.05 3MT, 0.1 M TBATFB/AcN) under potentiostatic conditions for 30 s (E_{app}=1.75 V) in 0.1 M H_2SO_4 and modified with a sol–gel containing Co-phthalocyanine layer. Data are shown for different dc voltages of 0.0 (▾), 0.4 (∩), 0.7 (▾), and 1.1 V (▾), respectively. *Dark symbols* represent log *Z* vs log *f* and *open symbols* represent phase angle vs log *f* relations. *Solid lines* represent simulated data based on the parameters of equivalent circuits of Fig. 5

poly(*p*-phenylene) [27] were reported earlier in the literature. The data obtained in the literature have been explained in terms of different 'equivalent circuits'. The choice of the circuit depended on the film thickness, the applied potential, and the nature of polymer. Electrochemical impedance plots often contain several time constants and a portion of one or more of their semicircles (in a typical Nyquist diagram) and a change in the phase angle in the intermediate frequency range (in a typical Bode plot) are usually seen. A comparison between data in Figs. 1 and 2 shows that 'fully' oxidized (as well as 'fully' reduced films, which are not shown in Figs. 1 and 2) films exhibited a proportional relation between log $|Z|$ and log f as the film is modified with the sol–gel layer. On the other hand, films subjected to a doping potential of ca. 0.4 V or higher showed a rather irregular behavior, namely, for the sol–gel modified polymer film. The previous observations are due to the fact that many factors contribute to the charge exchange at the polymer/electrolyte interface and, therefore, affect the EIS spectra. Among those factors is the hydrophobic nature of the polymer, the film morphology, the level of doping within the film, the applied potential, and the size of ions in contact with the polymer surface. Thus, the conducting polymer film can be considered as an anion exchanger in the oxidized state. A potential drop across the metal/film/electrolyte interface is established which depends on the chemical potentials of the anions/cations exchange between the polymer and electrolyte.

In the analysis of data, we will consider the constant electron transfer between the metallic substrate and the conducting polymer film. Moreover, the rate-determining step for the charge transport is the transition of the electron from one redox site to a neighboring one as was previously described [28]. This transition is also known as 'electron-hopping' process that has diffusion nature [29]. The charge diffusion coefficients, D_e, are of the order of 10^{-10}–10^{-13} cm^2 s^{-1}. A 'Warburg'-type diffusion impedance element is normally used to describe this charge-hopping process [29]. The rate-determining step in the case of poly(alkylthiophenes) is the electron movement from one polymer chain to another [30]. The kinetics of charge transfer in PMT/sol–gel(MPc) film is therefore similar to a redox polymer, but with relatively high ionic and low electronic conductivities. It might be important at this stage to separate the double layer charging of the metal–film interface from the interfacial oxidation–reduction of the polymer and the associated diffusion-type electron transport across the film. When the hybrid film is oxidized, its electronic conductivity will exceed that of the mobile counter-ions within the film matrix [31]. Therefore, when an electrical field is established within the film, ions migrate to reach equilibrium. The film behaves in this case as a porous metal with pores of limited depth and size. According to De Levie [32], the impedance of a one-dimensional cylindrical pore structure with an invariant interfacial impedance, Z_o, along the wall of the pores can be described by a transfer function. It is possible to correlate the data to 'modified' Randles circuits that are shown in Fig. 5a,b. In the following set of equations, the terms are described as follows: Z_p, $R_{\Omega,p}$, $Z_{w,p}$, r_p, and l_p are the impedance of a single pore, the electrolytic resistance, the impedance of the pore wall in the polymer film, the radius of pore, and the length of pore, respectively.

$$Z_p = \sqrt{R_{\Omega,p} Z_{w,p}} \coth \sqrt{\frac{R_{\Omega,p}}{Z_{w,p}}} \tag{3}$$

$$R_{\Omega,p} = \frac{l_p}{\sigma \pi r_p l_p} \tag{4}$$

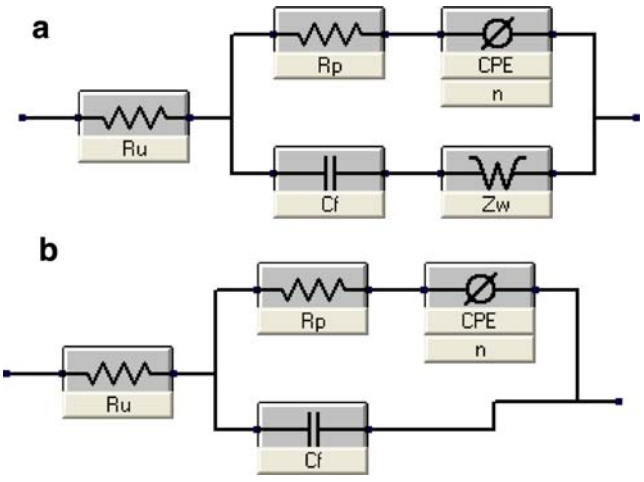

Fig. 5 Equivalent circuits used in the fit procedure of the impedance spectra of Figs. 1, 2, 3 and 4. The results were analyzed using Levenberg–Marquardt/Simplex algorithms based on a complex non-linear least-squares procedure

$$Z_{w,p} = \frac{Z_o}{2\pi r_p l_p} \tag{5}$$

The Warburg element, w (with a corresponding impedance of Z), in Fig. 5 represents a linear finite restricted diffusion of some species throughout the film, namely, anionic dopants. In the low-frequency region, the finite-length Warburg diffusion element (Z_D) is characterized by a diffusion time constant (τ_D), a diffusion pseudo-capacitance (C_D), and a diffusion resistance (R_D) that can be related by the following expression [33]:

$$Z_D = \frac{\left(\frac{\tau_D}{C_D}\right)\coth(jC\tau_D)^{1/2}}{(jwC_D)^{1/2}} \tag{6}$$

Several electrical circuits were initially tested by nonlinear least-squares fitting of the experimental impedance data. The equivalent circuit shown in Fig. 5 was found to give excellent fits down to frequencies including the low frequency corresponding to the bulk capacitance (at low frequency) of the polymer film. Our data also showed considerable deviation from the 90° capacitive lines at low frequencies. The model is composed of the solution resistance (R_u), the double layer capacitance (CPE), the low-frequency bulk-redox capacitance (C_f), and the 'classical' semi-infinite Warburg diffusion element (Z_D). The finite-length Warburg diffusion element Z_D is characterized by the diffusional time constant ($\hat{o}_D$), the diffusional pseudocapacitance (C_D), and the diffusion resistance (R_D) only in the low-frequency region.

The average error (χ^2) of the fits for 58 different impedance spectra of PMT and sol–gel modified PMT films at E_{applie} between 0 and 1.1 V was $\chi^2=4.3\times10^{-4}$.

We followed a nonlinear complex minimum square fitting protocol that is well established for studying polymeric systems to calculate the different electrochemical parameters [34]. The EIS parameters calculated for the different films tested in 0.1 M H_2SO_4 is given in Tables 1, 2, 3 and 4. It could be noticed that the differences in calculated values of R_u for each film changes with applied potential. This indicates that R_u does not represent the electrolytic resistance only. On the other hand, R_p is the charge transfer resistance associated with the interface between the film and electrolyte, whereas CPE, the constant phase element, represents charge accumulation at the interface that forms the interfacial double layer. The latter consideration assumes a flat configuration for the film, i.e., surface roughness is not taken into account. The value of CPE is eventually much larger than that corresponding to the double layer.

A careful inspection of the data shown in Tables 1, 2, 3 and 4 shows the following:

1. The value of R_u displayed a common trend for all polymer films. Thus, as the potential increases, the film is switched from a relatively insulating to a merely conductive one. As the applied potential approaches the oxidation of the polymer, R_u starts to decrease noticeably, indicating that the film is completely switched to the doped (conducting) state. A slight difference in these values is noticed between unmodified polymer film and those modified with the sol–gel or sol–gel(MPc) layers. This could be explained in terms of the conduction mechanism that involves ionic diffusion within the film and which is much accessed in case of PMT film vs the sol–gel-coated films.
2. The charge transfer resistance that is represented by R_p was found to be relatively high. This indicates that a charge transfer process at the polymer/electrolyte interface (that includes double layer) is not significant at the relatively lower end of the frequency. However, it will be difficult to obtain a full description of the

Table 1 EIS fitting data of polymer coated over Pt surface and tested in 0.1 M H_2SO_4

E_{appl} V	R_u 10^1 Ω cm^2	R_p 10^5 Ω cm^2	C_f 10^{-5} F cm^{-2}	Z_w 10^{-1} Ω cm^2 s$^{1/2}$	Q 10^3 S cm^{-2} s^n	n
0	4.1	8.3	1.1	10.8	9.3	0.83
0.4	1.8	2.6	4.3	9.2	8.4	0.74
0.7	1.8	0.19	44	2.4	4.6	0.62
1.1[a]	1.2	0.11	51	–	4.1	0.62

[a] The equivalent circuit of Fig. 5b was used for data analysis.

Table 2 EIS fitting data of polymer coated over Pt surface then modified by a sol–gel layer and tested in 0.1 M H_2SO_4

E_{appl} V	R_u 10^1 Ω cm^2	R_p 10^5 Ω cm^2	C_f 10^{-3} F cm^{-2}	Z_w 10^{-1} Ω cm^2 s$^{1/2}$	Q 10^4 S cm^{-2} s^n	n
0	7.4	8.7	5.8	6.3	1.4	0.87
0.4	5.7	3.7	0.56	4.2	0.62	0.72
0.7	2.1	1.1	0.13	1.3	0.21	0.73
1.1[a]	2.0	0.90	0.21	–	0.22	0.63

[a] The equivalent circuit of Fig. 5b was used for data analysis.

behavior of charge transfer within the double layer at the film/solution interface. It is obvious from the above discussion that the electron transport through the polymer chains is accompanied by ionic migration. The transport of ions through the double layer and particularly at the film/solution interface may be modeled as the charge/discharge of a capacitor. As the surface of the polymer is not ideally regular and the binding sites of ions to the polymer possess different energies, a capacitive component and constant phase elements have to be associated with the charge transfer resistance [35]. It is important to notice that there is an appreciable decrease in the values of R_p, which observed in the case of films modified with a sol–gel (MPc). Moreover, a progressive decrease in the R_p values was displayed as the applied potential increases. The charge transfer resistance is a measure of the facility of the exchange rate of charge at the interface [36]. The fact that the maximum value of electron transfer is reached as the film potential approaches its E_{ox} value indicates that a high ionic uptake predominates over the charge diffusion. We noticed a variation in CPE (Q) and the Warburg (Z_w) components for relatively thicker films maintained at relatively low applied potentials. It is more correct to indicate at this point that charge transfer resistance values cannot be considered solely as a measure for film conductivity with the change of the applied potential to the film.

Table 3 EIS fitting data of polymer coated over Pt surface then modified by a sol–gel layer containing Cu-phthalocyanine and tested in 0.1 M H_2SO_4

E_{appl} V	R_u 10^1 Ω cm^2	R_p 10^5 Ω cm^2	C_f 10^{-3} F cm^{-2}	Z_w 10^{-1} Ω cm^2 s$^{1/2}$	Q 10^4 S cm^{-2} s^n	n
0	1.1	8.1	4.3	4.7	5.2	0.85
0.4	2.5	1.5	0.10	4.1	0.38	0.58
0.7	2.4	0.3	0.72	6.8	1.2	0.68
1.1[a]	2.3	0.087	0.26	–	0.073	0.38

[a] The equivalent circuit of Fig. 5b was used for data analysis.

Table 4 EIS fitting data of polymer coated over Pt surface then modified by a sol–gel layer containing Co-phthalocyanine and tested in 0.1 M H_2SO_4

E_{appl} V	R_u 10^1 Ω cm^2	R_p 10^5 Ω cm^2	C_f 10^{-3} F cm^{-2}	Z_w 10^{-1} Ω cm^2 s$^{1/2}$	Q 10^4 S cm^{-2} s^n	n
0	1.2	0.34	1.4	7.0	7.5	0.79
0.4	1.4	0.24	0.6	5.2	0.95	0.97
0.7	2.4	0.059	0.050	0.096	0.39	0.93
1.1[a]	3.8	0.043	0.052	–	0.53	0.64

[a] Equivalent circuit of Fig. 5b was used for data analysis.

Other factors such as film channeling, morphology, electrolyte memory effect, type of monomer, and film modification would affect such variation.

3. It is clear that the CPE (Q) is associated with the polymer film capacitance, C_f, and depends on the applied potential and modification. Thus, the value of CPE (Q) decreases while that of C_f increases when comparing PMT with sol–gel-modified film. This finding shows the effect of hydrophobic nature of the film and its capacitive properties that has a major contribution on the applicability of these films in rechargeable batteries and electrocatalysis [41]. The polymer film possibly reaches a maximum C_f value as the value of E_{ox} is approached and in some cases when exceeding this value. The variation of the double layer capacitance produced by charge accumulation at the polymer/solution interface is related to the charge compensation taking place within the electrical double layer during the oxidation of the polymer. However, we would expect the results reported in this work to be relatively higher than those reported in the literature [27] due to the difference in estimation of thickness of the film and the method of its formation/modification. Moreover, the swelling of the film caused by the solvent/electrolyte interaction should have a remarkable effect on the values of CPE (Q).

In the case of the polymer modified with the sol–gel and sol–gel(MPc), the resulting polymer/inorganic hybrid has the following suggested structure: a relatively less dense and semi-porous film of an organic polymer covered with a sol–gel layer. The conductive polymer film is relatively thicker than that of the inorganic layer. This was estimated from the scanning electron microscopic experiments of the surface. In this respect, there is a good possibility of inter- and/or intra-cluster ionic migration through the modified film. A similar finding was suggested earlier [30] and recently [37] in the literature for other granular systems. We will consider the PMT/sol–gel interface as a heterogeneous layer, where individual grains in the inorganic layer are in

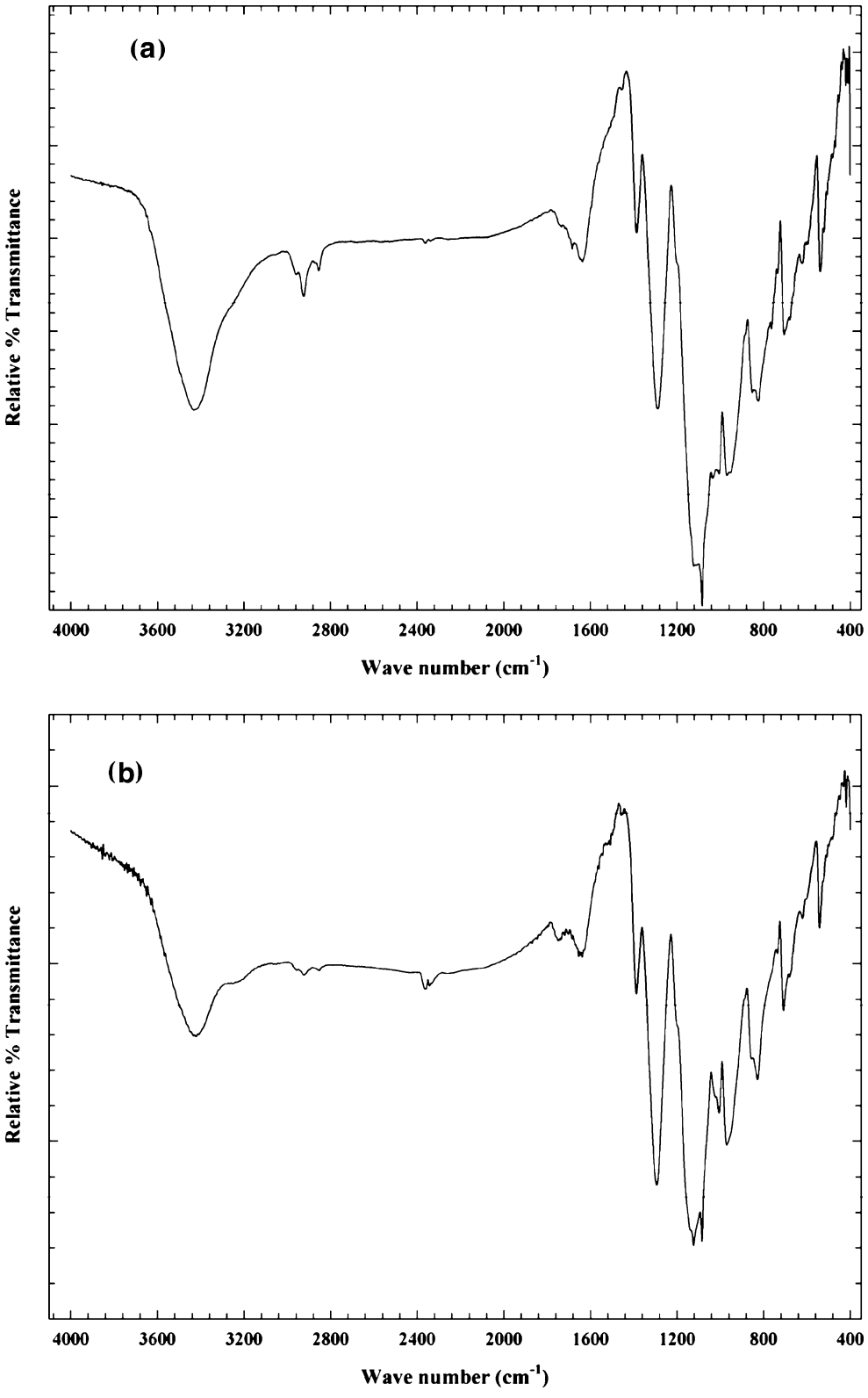

Fig. 6 **a** The FTIR spectrum of poly(3-methylthiophene) grown under a constant potential of E_{app}=1.8 V. **b** The FTIR spectrum of poly(3-methylthiophene) grown under a constant potential and covered with a layer of Co-phthalocyanine

contact with each other at the PMT/inorganic boundaries. Therefore, the ac response may be analyzed into two parallel or two series elements representing inter- and/or intra-granular and the film/electrolyte interfaces, respectively. The parallel model was assigned to relatively thin inorganic coating and the series one for the rather thicker layer. The capacitance associated with the presence of grain boundary regions is always larger than the bulk capacitance

of the film. This is because the grain boundary regions are thinner than the organic conducting film. In most cases, migration across grain boundaries is highly restricted and, therefore, the inter-grain resistances are larger than the internal resistance of the film despite the fact that grain boundaries are thinner. Two time constants (at least) should be observed for granular-containing films [38]. The first one at relatively high frequency is assigned to the bulk capacitance and bulk resistance due to intra-film ionic migration, and the second one expresses the capacitance and resistance associated with the grain boundary regions due to inter-cluster ionic migration. A charge transfer should be facilitated when the sol–gel bears the metal complex and results in the observed less R_p values. Thus, the Bode plots obtained at room temperature for the organic conducting polymer film hybridized with the inorganic layer were fitted using the $R_u(R_pC_f)$(CPE) (of Fig. 5b) or the $R_u(R_p/C_f\text{CPE}Z_w)$ (of Fig. 5a) equivalent circuit (Fig. 5). We were not able to model the data by any equivalent circuit that is composed entirely of frequency-independent components. The CPE (Q) is generally expressing the distribution of the current density along the polymer surface as a result of surface non-homogeneity. Tables 2, 3 and 4 show the analyzed data for polarization resistance, R_p, the Warburg element, Z_w, the film capacitance, C_f, and the interfacial resistance, R_u, values for platinum/polymer/inorganic system as calculated from Figs. 2, 3 and 4. The results display the effect of changing the modification from sol–gel to sol–gel(CuPc) and sol–gel(CoPc) films. The following observations could be drawn from the data of Tables 2, 3 and 4:

1. The ohmic resistance, R_u, associated with the modified film/electrolyte interface increased relatively when compared to the non-modified film, namely, when the applied potential increases. This indicates that the inter-cluster ionic migration was facilitated. The later observation is due to the ionic inclusion that increases as the applied potential approaches the oxidation potential of the system. It is also clear that as the applied positive potential decreases, the separation between inter- and/or intra-cluster ionic migration and the electronic conduction are hindered. In summary, when the inorganic phase was introduced into the polymer matrix, noticeable changes in impedance behavior as indicated in Figs. 2, 3 and 4 as well as in film morphology (as indicated in the SEM data section) were observed. Frequency dispersion is another factor contributing to the observed changes taking place in the intermediate frequency domains of the Bode plots of these films. This indicates a change in the conduction mode through the film. At the high-frequency region, the bulk capacitance associated with the dielectric polarization of the polymer chains caused by the alternating field starts to be effective. Moreover, as the frequency increases, the impedance of the bulk resistance (R_p) and capacitance (C_f) approach the same magnitude. Both resistance and capacitance of the bulk contribute significantly to the overall impedance.
2. At the relatively low-frequency ranges, C_f makes a negligible contribution to the impedance. The highest values for R_p and C_f were observed in the case of PMT/sol–gel.
3. The effect of introducing a MPc in the polymer film layer was reflected on the decrease in the respective values of R_u, R_p, and C_f. However, a noticeable increase in the value of C_f is noticed in this case when compared to the unmodified PMT film. One important aspect of the utilization of this type of materials is the charge storage capability and the facilitation of the reversible charge/discharge process. We observed an increase in charge storage capacity of the modified films of this class of conducting polymers with the applied potential. These materials were also used successfully as modified surfaces for the electrocatalytic conversion of H_2O_2 for fuel cells applications [41].

IR spectroscopic analyses of the polymer film and phthalocyanine-modified polymer films

The Fourier transform infrared spectroscopy (FTIR) spectrum of KBr-pressed pellet of PMT grown under a constant applied potential of 1,800 mV is shown in Fig. 6a. The number of scans collected at a resolution of 2 cm^{-1} and with an accuracy of 0.004 cm^{-1} were 32 for all samples. The results shown in Fig. 6a are in good agreement with those published earlier [39]. A series of principal absorption bands appear in the region from 540 to 850 cm^{-1}. Those bands are characteristic of the C–H out-of-plane vibrations. Three consecutive weak peaks appeared at 2,980, 2,925, and 2,863 cm^{-1}, assigned to aliphatic C–H stretching vibration bands. The band appearing at 1,390 cm^{-1}, which could be attributed to the ring stretching mode absorption vibration band at 1,293 cm^{-1}, is associated with methyl deformation. The ring stretching modes appeared at 1,560, 1,519, and 1,458 cm^{-1} [40]. The absorption mode of the aromatic C–H in plane deformation coupling with the skeletal vibration of aromatic ring appears at 1,083 cm^{-1}. A noticeable band at 826 cm^{-1} is assigned to the aromatic C–H out-of-plane deformation mode.

Figure 6b shows the FTIR spectra of KBr-pressed pellet of PMT/sol–gel(CoPc). The composite film was left to dry and finally rinsed with acetonitrile. The IR spectra of the

Table 5 Elemental microanalysis and empirical formula for PMT and PMT/phthalocyanine films

Elemental microanalysis								
Film[a]	C, %	H, %	N, %	S, %	O, %	Cu, %	Co, %	Empirical formula
PMT	42.98	3.96	0.41	22.19	30.46	–	–	$C_{5.1}H_{5.8}S_{1.0}N_{0.042}O_{2.7}$
PMT/CuPc	47.15	3.41	0.90	23.05	22.70	2.78	–	$C_{5.4}H_{4.7}S_{1.0}N_{0.089}O_{1.9}Cu_{0.06}$
PMT/CoPc	40.75	3.58	0.55	20.11	31.56	–	3.42	$C_{5.4}H_{5.7}S_{1.0}N_{0.062}O_{3.1}Cu_{0.092}$

[a] PMT was prepared under constant applied potential, and for the second and third films the phthalocyanine layer was applied according to the second method as described in the "Experimental" section.

PMT/sol–gel(CuPc) and PMT/sol–gel(CoPc) films are basically similar. The IR spectra of Fig. 6b display basically the same band characteristics for the PMT as indicated previously in Fig. 6a. However, several bands appear distinctly in the spectra of Fig. 6b which indicate the presence of the Pc moiety. Thus, the characteristic IR band at 1,006 cm^{-1} is interpreted as C–N (pyrrole) in-plane bending vibration for metal-free Pc and to N–H in-plane or out-of-plane bending mode. The new absorption bands appearing at 1,120 and 670 cm^{-1} were attributed to Pc skeletal vibration modes.

The aforementioned interpretations showed and proved that the aromatic structure of the hetero-arylene was maintained in the resulting polymer chains as expected. Moreover, the Pc moieties existed within the film matrix when modified films were analyzed. This is in good agreement with the data obtained from elemental analysis that showed the presence of Co and Cu metals within the modified film matrices.

Elemental analysis

Based on the stoichiometry of the oxidative polymerization reaction, the polymerization of 1.0 g of 3-methylthiophene yields theoretically 0.89 g of PMT. The apparent yield of PMT under the standard polymerization conditions approaches 100% within the experimental error. We will also assume that the current efficiency for the electropolymerization is almost 100%. The elemental analysis indicates that doping ions from the supporting electrolyte, such as the bulky tetra-butyl ammonium or tetra-fluoroborate counter ions (not shown in Table 5), are possibly present in the film.

Shown in Table 5 are the differences in elemental composition of PMT prepared without modification and those modified with MPc. The results of elemental analysis clearly indicate the presence of oxygen in PMT (in the range of 2 to 3%). This may be due to bound water molecules or, more likely, to partial oxidation of the polymer chains. The presence of nitrogen is partly due to the residual tetra-butyl ammonium counter ions produced during the redox cycles. However, the relative percentage of nitrogen in the film rises generally for the film modified with the phthalocyanine layer. The relative participation of Cu and Co in the PMT generally causes the relative increase in nitrogen and oxygen content in the films (with the exception of the Cu-phthalocyanine-containing sample that rather showed decreases in hydrogen content).

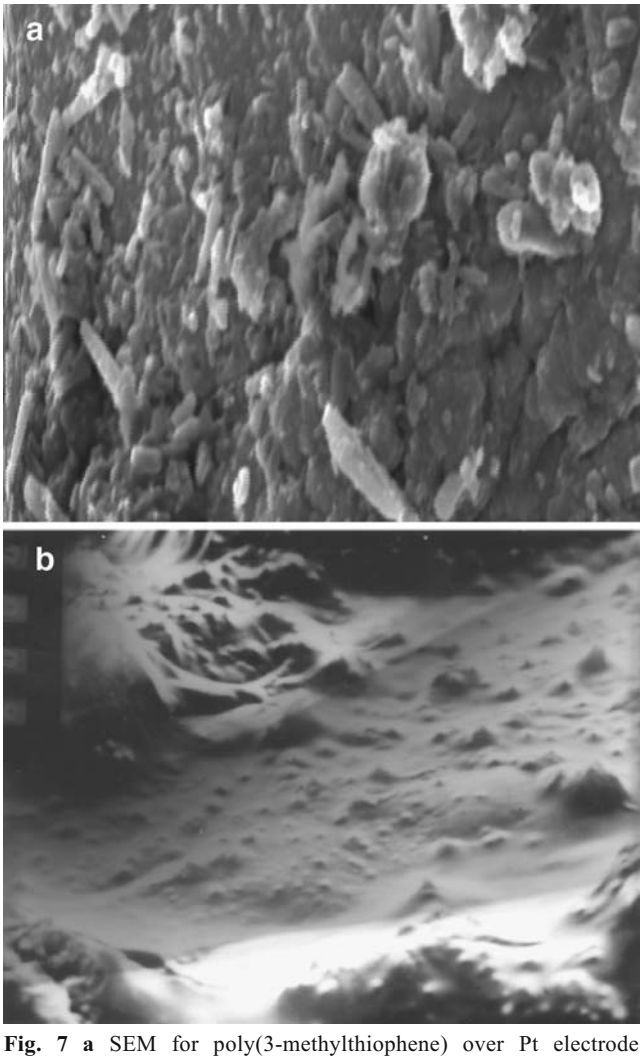

Fig. 7 **a** SEM for poly(3-methylthiophene) over Pt electrode (E_{app}=1.8 V for 20 s; magnification ×1,500; thickness of the layer 200 Å. **b** SEM for poly(3-methylthiophene) modified with Cu-phthalocyanine sol–gel (magnification ×1,500)

Scanning electron microscope

In this section, the morphological structure of the polymer films were studied and compared. The following films were examined: PMT and PMT/sol–gel(CuPc).

In general, five-membered heterocycles (such as thiophenes, pyrroles, furans, and selenophenes) electropolymerize through 2–5 coupling. This should result in a highly ordered chain structure provided that the coplanarity of the units within the chains is also respected. In this respect and taking into account the controlled conditions of synthesis, such as monomer/electrolyte concentration, solvent, applied potential, etc., planning the number and extent of substitution in the 5 (β)-positions in the monomeric compound should more importantly result in a more likely ordered polymeric film. It is important to mention that morphological surface defects may result from the unlikely 2–5 (α–β) coupling during the propagation step or extended film thickening. Figure 7a shows the SEM picture of the solution side of a 200-Å-thick film of PMT. As can be noticed from Fig. 7a, the surface is typical for undoped PMT films. In this figure, the surface looks homogeneous and shows some roughness due to the platinum substrate and relatively thin film. The compactness of the structure is attributed partially to the removal of the dopant anions and to conformational changes due to polymer chain rearrangement. Figure 7b shows the SEM of a PMT/sol–gel(CuPc) film. In this case, the surface appears to have more amorphous structures. This is attributed to the deposition of the inorganic moiety over the conducting polymer layer. At this level of magnification, no pores were identified; however, different packing distributions of the film are noticed. The surface shows relatively higher homogeneity compared to the PMT unmodified film. Due to the effect of blending that is caused by heating, the surface is also shown with some particles appearing sub-wigged into the film. A defect in the surface that was caused by the mount of the SEM holder is noticed at the upper left corner of the picture. All pictures were taken at a magnification of ×1,500 that corresponds to a scale factor of 2.

Conclusion

The modification of poly(3-methyl thiophene) films with a sol–gel layer containing Cu- or Co-Pc resulted in a relatively less dense and semi-porous film. The capacitance of the film increases accordingly and its impedance decreases with the inclusion of the MPcs centers. In particular, charge transfer resistance, R_p, reached its minimum as the oxidation potential of the modified film was reached. It could be concluded that the conductive polymer layer is contributing to the charge transfer process with the presence of the sol–gel(MPc) layer. The film morphology and its possible hydrophobic nature contribute to the differences obtained of the EIS data. The PMT/sol–gel interface is a heterogeneous layer and the ac response was described as two elements representing the inter- and/or intra-granular and the film/electrolyte interfaces system. The IR band at 1,006 cm^{-1} ascertained the presence of the Pc moiety in the film and confirms the elemental analysis.

Acknowledgments This work was performed with partial financial support from 'The Young Researchers' Program' of the University of Cairo (Office of the Vice President for Graduate Studies and Research). We are indebted to Prof. T.H. Ridgway and Prof. W.R Heineman of the University of Cincinnati (OH, USA) for allowing us to use some electrochemical equipment.

References

1. Mark HB Jr, Rubinson JF, Krotine J, Vaughn W, Goldschmidt M (2000) Electrochim Acta 45:4309
2. Li X, Zhang S, Sun C (2003) J Electroanal Chem 553:139
3. Varela H, Bruno RL, Torresi RM (2003) Polymer 44:5369
4. Jiang J, Kucernak A (200) Electrochim Acta 45:2227
5. Brylev O, Alloin F, Duclot M, Souquet JL, Sanchez JY (2003) Electrochim Acta 48:1953
6. Radhakrishnan S, Unde S (1999) Thin Solid Films 347:229
7. Ballarina B, Zanardib C, Schenettib L, Seeberb R, Hidalgo JL, de Cisnerosc H (2003) Synth Met 139:29
8. Apetrei C, Rodriýguez-Méndez ML, Parra V, Gutierrez F, de Saja JA (2004) Sens Actuators B Chem 103:145
9. Xu F, Li H, Cross J, Guarr TF (1994) J Electroanal Chem 368:221
10. Sorokin AB, Buisson P, Pierre AC (2001) Microporous Mesoporous Mater 46:87
11. Vorotyntsev MA, Daikhin LI, Levi MD (1994) J Electroanal Chem 364:37
12. Venkatachalam S (1989) Polymer 30:1633
13. Refaey SAM (2004) Synth Met 140:87
14. Chao F, Costa M, Tian C (1993) Synth Met 53:127
15. Levi MD, Gofer Y, Aurbach D, Berlin A (2004) Electrochim Acta 49:433
16. Gabrielli C, Keddam M (1996) Electrochim Acta 41:957
17. Roncali J (1997) Chem Rev 97:173
18. Galal A (1991) Preparation, characterization and applications of some poly(heteroarylenes). Ph.D. thesis, University of Cincinnati, OH, USA
19. Brédas JL, Street GB (1985) Acc Chem Res 18:309
20. Lippe J, Holzer R (1991) Synth Met 43:2927
21. Fosset B, Amatore CA, Bartelt JE, Michael AC, Wightman MR (1991) Anal Chem 63:306
22. Popkirov GS, Barsoukove E (1995) J Electroanal Chem 383:155
23. Pickup PG (1990) J Chem Soc Faraday Trans 86:3631
24. Del Valle MA, Cury P, Schrebler R (2002) Electrochim Acta 48:397
25. Garcia-Belmonte G, Bisquert J (2002) Electrochim Acta 47:4263
26. Chen WC, Weu TC, Hu CC, Gopalan A (2002) Electrochim Acta 47:1305
27. Dubois M, Billand D (2002) Electrochim Acta 47:4459

28. Andrieux CP, Haas O, Savéant JM (1986) J Am Chem Soc 108:8175
29. Nieto F Jr, Tucceri RI (1996) J Electroanal Chem 416:1
30. Roth HK, Krinichnyi VI (2003) Synth Met 137:1432
31. Visy C, Kankare J (2000) Electrochim Acta 45:1811
32. De Levie R, Delehay P (eds) (1967) Advances in electrochemistry and electrochemical engineering, vol 6. Interscience, New York, p 329
33. Bobacka J, Lewenstam A, Ivaska A (2000) J Electroanal Chem 489:17
34. CMS 300 Software, version 2.4a (1996) Gamry Instruments, USA
35. Tanguy J, Baudoin JL, Chao F, Costa M (1992) Electrochim Acta 37:1417
36. Bard AJ, Faulkner LR (2001) Electrochemical methods, fundamentals and applications, 2nd edn. Wiley, New York, pp 115–132
37. Chen YJ, Zhang XY, Li YZ (2003) J Magn Magn Mater 267:152
38. Bruce PG, West AR (1983) J Electrochem Soc 130:662
39. Holdcroft S, Funt BL (1988) J Electroanal Chem 240:89
40. Uff BC (1986) In: Katritz AR, Rees CW (eds) Comprehensive heterocyclic chemistry, vol 2A. Pergamon, Oxford, pp 17, 18, 738
41. Galal A, Darwish SA, Ahmed RA (2006) J Solid State Electrochem (in press)